A Simplified Kinematic Method for 3D Limit Analysis

James P. Hambleton[1, a *] and Scott W. Sloan[1,b]

[1]ARC Centre of Excellence for Geotechnical Science and Engineering, The University of Newcastle, Callaghan, NSW 2308, Australia

[a]James.Hambleton@Newcastle.edu.au, [b]Scott.Sloan@Newcastle.edu.au

*corresponding author

Keywords: Limit analysis, kinematic method, upper bound, three-dimensional, optimization

Abstract. The kinematic (upper bound) method of limit analysis is a powerful technique for evaluating rigorous bounds on limit loads that are often very close to the true limit load. While generalized computational techniques for two-dimensional (e.g., plane strain) problems are well established, methods applicable to three-dimensional problems are relatively underdeveloped and underutilized, due in large part to the cumbersome nature of the calculations for analytical solutions and the large computation times required for numerical approaches. This paper proposes a simple formulation for three-dimensional limit analysis that considers material obeying the Mohr-Coulomb yield condition and collapse mechanisms consisting of sliding rigid blocks separated by planar velocity discontinuities. A key advantage of the approach is its reliance on a minimal number of unknowns, which can dramatically reduce processing time. The paper focuses specifically on tetrahedral blocks, although extension to alternative geometries is straightforward. For an arbitrary but fixed arrangement of blocks, the procedure for computing the unknown block velocities that yield the least upper bound is expressed as a second-order cone programming problem that can be easily solved using widely available optimization codes. The paper concludes with a simple example and remarks regarding extensions of the work.

Introduction

Among available methods for calculating limit loads on engineering structures, which include limit analysis, limit equilibrium, slip-line theory (method of characteristics), and the finite element method, limit analysis holds the appeal of being simultaneously rigorous and highly efficient. Moreover, closed-form analytical solutions often can be obtained [1]. Abundant literature can be found on the subject of analytical, semi-analytical and purely numerical approaches for assessing lower and upper bounds for two-dimensional problems, which consider either a state of plane strain or plain stress. By comparison, methods for analyzing three-dimensional problem are scarce. Simple translational or rotational velocity fields often provide reasonable analytical or semi-analytical upper bound solutions, as evidenced in the work of Shield and Drucker [2], Drescher [3], Michalowski [4], and others. Generalized finite element limit analysis techniques have also been developed [5-8], although their application in the solution of practical problems has been limited by the difficulty of their implementation and the computational effort needed to obtain a satisfactory result, given the large number of degrees of freedom required.

This paper presents a new kinematic formulation for three-dimensional limit analysis premised on optimizing collapse mechanisms consisting of sliding rigid blocks separating by infinitesimally thin zones of shearing. The purpose of developing the technique is to strike a balance between simplified solution techniques (e.g., [2-4]), which often give satisfactory results but only through tedious hand calculations, and finite element limit analysis procedures (e.g., [5-8], which are computational intensive and in many instances needlessly complex. The approach is developed for a material obeying the Mohr-Coulomb yield criterion, for which the relevant material parameters are the friction angle ϕ and cohesion c.

Kinematic method of limit analysis

The kinematic theorem of limit analysis states that the limit load computed from any kinematically admissible velocity field, or collapse mechanism, provides a rigorous bound on the true limit load. A kinematically admissible velocity field is one that (1) everywhere satisfies the plastic flow rule and (2) satisfies boundary conditions. The calculated limit load is an upper bound for loads inducing collapse and a lower bound for loads resisting collapse. Assuming the load induces collapse and takes the form of a traction applied over part of the boundary, the upper bound is assessed through the following balance of energy, which equates the rate of dissipation due to plastic deformation $\dot{d}$, integrated over the volume V of the kinematically admissible mechanism, to the rate of work due to external loads:

$$\int_V \dot{d}\left(\dot{\boldsymbol{\varepsilon}}\right) dV = \int_S \mathbf{t}\cdot\mathbf{v}dS + \int_{S^*} \mathbf{t}^*\cdot\mathbf{v}dS + \int_V \boldsymbol{\gamma}\cdot\mathbf{v}dV \,. \tag{1}$$

In Eq. (1), the rate of dissipation per unit volume $\dot{d}$ varies as a function of the plastic strain rate $\dot{\boldsymbol{\varepsilon}}$, which is, in turn, a function of the velocity $\mathbf{v} = [v_x\ v_y\ v_z]^T$. The external loads appearing on the right-hand side of Eq. (1) take the form of (1) the tractions $\mathbf{t}$ representing the unknown limit load over the boundary S, (2) fixed tractions $\mathbf{t}^*$, such as surcharge, acting over the boundary S^*, and (3) body forces $\boldsymbol{\gamma} = [\gamma_x\ \gamma_y\ \gamma_z]^T$.

One of the simplest means for implementing the kinematic method (cf. [1]) is to assume a velocity field composed of undeformed regions that undergo simple translational motion (i.e., rigid blocks) separated by thin zones of shearing, represented as lines across which the velocity undergoes a jump. These velocity jumps, or so-called velocity discontinuities, are kinematically admissible for a translational velocity field if they are straight lines (2D) or planes (3D) and if they satisify the following jump condition [1]:

$$\left\|\Delta\mathbf{v}_n\right\| = \left\|\Delta\mathbf{v}_t\right\|\tan\phi\,, \tag{2}$$

where

$$\left\|\Delta\mathbf{v}_n\right\| = \left|\Delta\mathbf{v}\cdot\mathbf{n}\right|, \tag{3}$$

$$\left\|\Delta\mathbf{v}_t\right\| = \sqrt{\Delta\mathbf{v}^T\Delta\mathbf{v} - \left(\Delta\mathbf{v}\cdot\mathbf{n}\right)^2}\,, \tag{4}$$

$$\Delta\mathbf{v} = \mathbf{v}_+ - \mathbf{v}_-\,. \tag{5}$$

In Eqs. (3)-(5), $\mathbf{n}$ denotes the unit vector normal to the discontinuity, and the quantities $\mathbf{v}_+$ and $\mathbf{v}_-$ denote the velocities on the "positive" and "negative" sides of the discontinuity, respectively. The "positive" side is associated with direction of the unit normal vector $\mathbf{n}$. Along each velocity discontinuity the total dissipation $\dot{D}$, obtained through integration of $\dot{d}$, is calculated as

$$\dot{D} = cA\left\|\Delta\mathbf{v}_t\right\|, \tag{6}$$

where A is the area of discontinuity (or length times an appropriate width in 2D). Upon completing the integration in Eq. (1) for an assumed arrangement of rigid blocks, the operational variables become the fixed point loads $\mathbf{P}^* = [\,P_x^*\ P_y^*\ P_z^*\,]^T$ acting on the blocks, and the final expression for the limit load P_u takes the form

$$P_u = \frac{1}{v_0}\left[\sum_{i=1}^{N_D}\dot{D}_i - \sum_{j=1}^{N_B}\left(\mathbf{P}_j^* \cdot \mathbf{v}_j\right)\right]. \tag{7}$$

In Eq. (7), the index i designates each velocity discontinuity (i = 1,2,…,N_D), and j indicates each rigid block (j = 1,2,…,N_B). The variable v_0 denotes the imposed reference velocity that gives an appropriate measure of the rate of work done by the limit load P_u (i.e., the work conjugate), typically selected as unity for convenience. Body forces γ_i can also be included in Eq. (7) by adding the force vector $\boldsymbol{\gamma}_j V_j$, where V_j is volume of block j, to $\mathbf{P}_j^*$.

Numerical formulation

One of the simplest conceivable procedures for computing a limit load using the kinematic method consists of first assuming a particular arrangement of blocks and then evaluating a set of velocities $\mathbf{v}_j$ (j = 1,2,…,N_B) that either minimizes or maximizes the limit load expressed in Eq. (7), subject to the jump conditions given by Eq. (2). For loads inducing collapse, which correspond to an upper bound, the task is to minimize Eq. (7), whereas the best lower bound for loads resisting collapse is obtained through maximization. Assuming the load is an upper bound, this section outlines a straightforward numerical procedure for completing this optimization for mechanisms consisting of tetrahedral blocks, for which the planar velocity discontinuities are the triangular regions formed between adjacent blocks.

Figure 1 schematically depicts two tetrahedral blocks sharing a common face OAB. For clarity, the blocks are separated, thus creating an additional but coincident set of points O′A′B′. The coordinates of points O, A, and B are specified by position vectors $\mathbf{x}_O$, $\mathbf{x}_A$, and $\mathbf{x}_B$, from which the two vectors $\mathbf{r}_A = \mathbf{x}_A - \mathbf{x}_O$ and $\mathbf{r}_B = \mathbf{x}_B - \mathbf{x}_O$ spanning the plane OAB are constructed. The unit normal vector $\mathbf{n}$ and area A can then be expressed as

$$\mathbf{n} = \frac{\mathbf{r}_A \times \mathbf{r}_B}{\left\|\mathbf{r}_A \times \mathbf{r}_B\right\|}, \quad A = \frac{1}{2}\left\|\mathbf{r}_A \times \mathbf{r}_B\right\| \tag{8}$$

Figure 1 depicts the unit normal $\mathbf{n}$, as well as the velocities $\mathbf{v}_+$ and $\mathbf{v}_-$ in adjacent blocks. Upon considering all discontinuities in the mechanism and the corresponding quantities $\mathbf{n}_i$ and A_i (i = 1,2,…,N_D), the following optimization problem arises:

$$\begin{aligned} &\text{minimize} \quad P_u = \frac{1}{v_0}\left[\sum_{i=1}^{N_D} cA_i \left\|\Delta\mathbf{v}_{t,i}\right\| - \sum_{j=1}^{N_B}\left(\mathbf{P}_j^* \cdot \mathbf{v}_j\right)\right] \\ &\text{subject to} \quad \left\|\Delta\mathbf{v}_{n,i}\right\| = \left\|\Delta\mathbf{v}_{t,i}\right\| \tan\phi, \; i = 1,2,...,N_D \\ &\qquad\qquad\; f_k\left(\mathbf{v}_k\right) = 0, \; k = 1,2,...,N_{BC} \end{aligned} \tag{9}$$

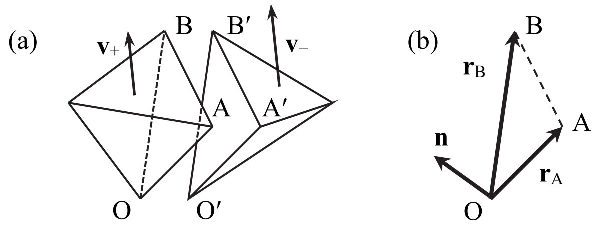

Fig. 1 Velocity discontinuity between two adjacent tetrahedral blocks: (a) local vertices (nodes) and velocities and (b) local position and normal vectors

In Eq. (9), the indices i and j denote quantities associated with the i^{th} discontinuity or j^{th} block (i = 1,2,…,N_D; j = 1,2,…,N_B), respectively. The functions f_k represent the conditions required to enforce kinematically admissible boundary conditions over the block faces on boundaries, and these are designated by k = 1,2,…,N_{BC}. These constraints are discussed in further detail below, observing that standard forms are articulated in greater detail elsewhere (e.g., [8]).

Equation (9) does not take the form of a standard mathematical programming problem due to the expressions involving the magnitude of the velocity jumps $\left\|\Delta\mathbf{v}_{t,i}\right\|$ and $\left\|\Delta\mathbf{v}_{n,i}\right\|$ (see Eqs. (3)-(4)). However, with some manipulation, Eq. (9) can be recast as a standard conic programming problem. The key step is to express each velocity jump $\Delta\mathbf{v}_{t,i}$ in terms of a local basis that aligns with the discontinuity. In particular, the components of $\Delta\mathbf{v}_{t,i}$ are transformed to a set of mutually orthogonal basis vectors $\mathbf{s}_i$, $\mathbf{t}_i$, and $\mathbf{n}_i$, where $\mathbf{s}_i$ and $\mathbf{t}_i$ are any two orthogonal unit vectors spanning the plane of the i^{th} velocity discontinuity, such that

$$\left\|\Delta\mathbf{v}_{t,i}\right\| = \lambda_i = \sqrt{\Delta v_{s,i}^2 + \Delta v_{t,i}^2}\,, \tag{10}$$

$$\left\|\Delta\mathbf{v}_{n,i}\right\| = \sqrt{\Delta v_{n,i}^2}\,, \tag{11}$$

where

$$\Delta v_{s,i} = \Delta\mathbf{v}_i\cdot\mathbf{s}_i\,,\; \Delta v_{t,i} = \Delta\mathbf{v}_i\cdot\mathbf{t}_i\,,\; \Delta v_{n,i} = \Delta\mathbf{v}_i\cdot\mathbf{n}_i\,. \tag{12}$$

With the aid of Eqs. (10)-(12), the expressions for the limit load and the jump conditions become, respectively,

$$P_u = \frac{1}{v_0}\left[\sum_{i=1}^{N_D} cA_i\lambda_i - \sum_{j=1}^{N_B}\left(\mathbf{P}_j^*\cdot\mathbf{v}_j\right)\right],\; \Delta v_{n,i} = \lambda_i\tan\phi \tag{13}$$

Finally, rather than directly utilizing the strict equalities of Eqs. (10) and (13), the constants λ_i are replaced with the dummy variables μ_i (i = 1,2,…,N_D), which obey the inequality

$$\mu_i \geq \sqrt{\Delta v_{s,i}^2 + \Delta v_{t,i}^2}\,. \tag{14}$$

This results in the following optimization problem:

$$\begin{aligned} &\text{minimize} && P_u = \frac{1}{v_0}\left[\sum_{i=1}^{N_D} cA_i\mu_i - \sum_{j=1}^{N_B}\left(\mathbf{P}_j^*\cdot\mathbf{v}_j\right)\right] \\ &\text{subject to} && \Delta v_{n,i} = \mu_i\tan\phi,\; \Delta v_{s,i} = \Delta\mathbf{v}_i\cdot\mathbf{s}_i,\; \Delta v_{t,i} = \Delta\mathbf{v}_i\cdot\mathbf{t}_i,\; \Delta v_{n,i} = \Delta\mathbf{v}_i\cdot\mathbf{n}_i,\; i = 1,2,...,N_D \\ &&& \mathbf{v}_k\cdot\mathbf{s}_k = v_{s,k}^*,\; \mathbf{v}_k\cdot\mathbf{t}_k = v_{t,k}^*,\; \mathbf{v}_k\cdot\mathbf{n}_k = v_{n,k}^*,\; k = 1,2,...,N_{BC} \\ &&& \mu_i \geq \sqrt{\Delta v_{s,i}^2 + \Delta v_{t,i}^2},\; i = 1,2,...,N_D \end{aligned} \tag{15}$$

Equations (9) and (15) differ in that the constraints required to enforce kinematically admissible boundary conditions, $f_k(\mathbf{v}_k) = 0$, are expressed explicitly in Eq. (15) in terms of the basis vectors $\mathbf{s}_k$, $\mathbf{t}_k$, and $\mathbf{n}_k$ for each face k (k = 1,2,…,N_{BC}) over which boundary conditions are specified. With these constraints, the boundary conditions can be conveniently enforced in terms of specified tangential velocity components, $v_{s,k}^*$ and $v_{t,k}^*$, and specified normal components, $v_{n,k}^*$.

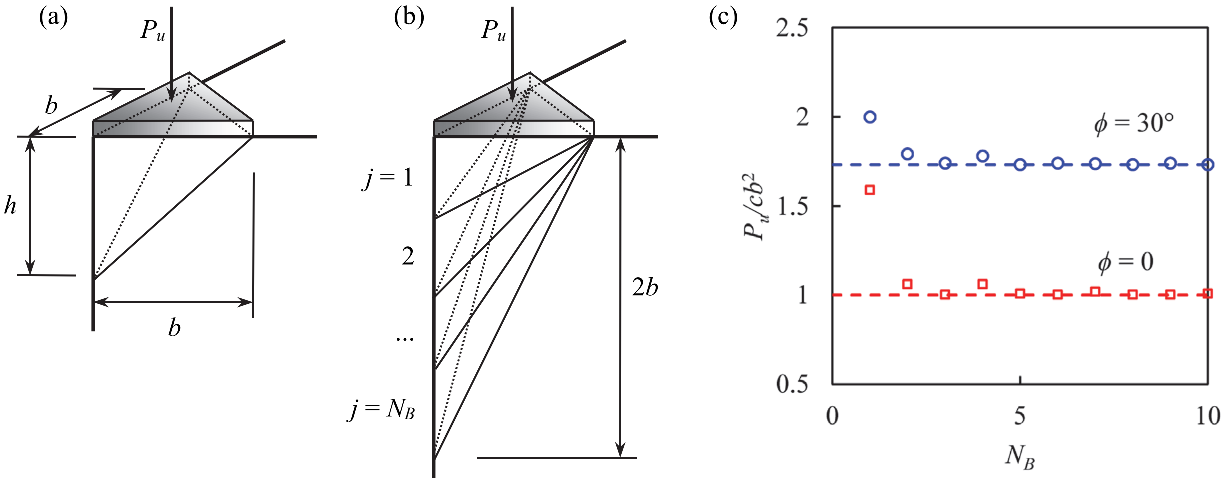

Fig. 2 Example problem used for verification: (a) problem definition and assumed single-block failure mechanism for the analytical solution; (b) arrangement of blocks assumed in the proposed numerical formulation; (c) computed limit loads compared with analytical solutions (dashed lines)

The final set of constraints appearing in Eq. (15) are referred to as "second-order conic constraints", and the overall optimization problem falls within the class of second-order cone programming problems. Upon formulating the problem in this way, the expression for the limit load appearing as the objective function in Eq. (15), as well as the jump conditions expressed in the set of constraints, are not specified as strict equalities. Rather, equality is achieved through the process of minimization, since the positive variables μ_i appearing in the objective function are least when $\lambda_i = \mu_i$ for all $i = 1,2,\ldots,N_D$. Upon completing the optimization process, one can easily verify that the equalities from the original optimization problem (e.g., Eq. (9)) are also satisfied, thus ensuring a rigorous upper bound.

The second-order cone programming problem of Eq. (15) can be solved using any of a number of freely or commercially available software packages. The example considered in the following section was completed using a simple MATLAB script interfacing with the MOSEK optimization toolbox.

Example

Figure 2 depicts the example problem used to verify the proposed numerical formulation. The example considers a triangular rigid footing placed at the corner of a rectangular prism of weightless material. The two edges of the footing at right angles to one another have the same length b, as depicted in Fig. 2(a). The interface between the footing and the underlying material is taken to be smooth, and the limit load to be determined is the normal force P_u on the footing at collapse. For this simple example, the following analytical solution can be derived assuming the single-block collapse mechanism shown in Fig. 2(a):

$$\frac{P_u}{cb^2} = \frac{\cos\phi}{1-\sin\phi},\ \frac{h}{b} = \frac{\sqrt{2}}{2}\tan\left(\frac{\pi}{4}+\frac{\phi}{2}\right). \tag{16}$$

Figure 2(b) shows the arrangement of rigid blocks used in verifying the proposed numerical approach. A fixed arrangement of contiguous blocks extending to depth $2b$ into the stratum is assumed, and the region is subdivided at regular intervals into a total number of blocks N_B (see Fig. 2(b)). In this arrangement, the locations of potential velocity discontinuities are defined uniquely by N_B, with larger values of N_B enabling greater refinement in the selection of the optimal location. Upon solving Eq. (15) for a particular value of N_B, one can confirm that sliding occurs only along the velocity discontinuity closest to the plane defined by optimal depth *h*, although sliding is free to occur along any of the planes within the assembly. The limit load computed for various choices of N_B are plotted in Fig. 2(c), where it is seen for two different values of ϕ that the numerical predictions rapidly converge to the analytical solution, with the error dropping below 1% in both cases for $N_B \geq 5$. In each case, the result was obtained in a fraction of a second on a PC with an Intel Core i7-4790K CPU clocked at 4.0 GHz. As an indicator of the efficiency of the approach, the optimization process was also completed assuming $N_B = 10^4$, and even for such a large number of blocks the optimization process was completed in approximately 0.3 seconds using MOSEK.

Concluding remarks

The paper presents a new numerical technique for assessing limit loads for three-dimensional problems based on the kinematic method of limit analysis and an assumed collapse mechanism consisting of sliding tetrahedral blocks separated by velocity discontinuities. A major advantage of the formulation is that it relies on a small number of unknowns, thus allowing for rapid computation of rigorous upper bounds for an arbitrary but fixed arrangement of blocks for which a kinematically admissible velocity field can be found. Ongoing work focuses automating the process of optimizing the location of the velocity discontinuities, which can be achieved, for example, using a variant of the perturbation scheme developed by the authors for two-dimensional problems [9].

Acknowledgements

The authors gratefully acknowledge financial support provided by the Australian Research Council through the ARC Centre of Excellence for Geotechnical Science and Engineering (CE110001009).

References

[1] W.F. Chen, Limit Analysis and Soil Plasticity, Elsevier, Amsterdam, 1975.

[2] R.T. Shield, D.C. Drucker, The application of limit analysis to punch-indentation problems, J. Appl. Mech. 20 (1953) 453-460.

[3] A. Drescher, Analytical methods in limit analysis, Ingenieur-Archiv 59 (1989) 138-147.

[4] R.L. Michalowski, Upper-bound load estimates on square and rectangular footings, Géotechnique 51 (2001) 787-798.

[5] K. Krabbenhøft, A.V. Lyamin, S.W. Sloan, Three-dimensional Mohr-Coulomb limit analysis using semidefinite programming, Commun. Numer. Meth. Engng. 24 (2008) 1107-1119.

[6] M. Vicente da Silva, A.N. Antão, Upper bound limit analysis with a parallel mixed finite element formulation, Int. J. Solids Struct. 45 (2008) 5788-5804.

[7] C.M. Martin, A. Makrodimopoulos, Finite-element limit analysis of Mohr-Coulomb materials in 3D using semidefinite programming, J. Eng. Mech. 134 (2008) 339-347.

[8] S.W. Sloan, Geotechnical stability analysis, Géotechnique 63 (2013) 531-572.

[9] J.P. Hambleton, S.W. Sloan, A perturbation method for optimization of rigid block mechanisms in the kinematic method of limit analysis, Computers Geotech. 48 (2013) 260-271.